Hydroperoxy-10,12-Octadecadienoic Acid Stimulates Cytochrome P450 3A Protein Aggregation by a Mechanism That Is Inhibited by Substrate†

Amy L. Kimzey,‡ Karl K. Weitz,‡ F. Peter Guengerich,§ and Richard C. Zangar*,‡

Pacific Northwest National Laboratory, Richland, Washington, 99352, and Department of Biochemistry and Center in Molecular Toxicology, Vanderbilt University School of Medicine, Nashville, Tennessee 37232-0146

Received June 12, 2003; Revised Manuscript Received August 13, 2003

ABSTRACT: We recently demonstrated that microsomes from nicardipine-treated rats will form cytochrome P450 3A (CYP3A) aggregates when incubated at 37 °C. CYP3A substrates inhibited the protein aggregation and subsequent degradation, suggesting that this process is important in substrate-mediated stabilization of CYP3A. In this paper, we demonstrate that oxidative stress is a key factor in the formation of CYP3A aggregates in incubated microsomes and in a reconstituted system with purified enzymes. Our data further suggest that the effects of oxidative stress are mediated by lipid hydroperoxides, which are efficiently metabolized by CYP3A. In the presence of substrate, the CYP3A-mediated lipid hydroperoxide metabolism is inhibited along with the associated protein aggregation. Therefore, these studies provide a mechanistic model of why CYP3A has a relatively short half-life and how substrates stabilize CYP3A.

P450s[1] constitute a superfamily of heme-containing enzymes that catalyze a wide variety of biochemical reactions (*1*). The P450 3A subfamily (CYP3A) members are transmembrane proteins expressed at the highest levels in the ER of the liver and intestine. CYP3A has been reported to metabolize approximately 50% of prescribed drugs and to catabolize many endogenous lipophilic compounds such as testosterone (*2*). Changes in CYP3A activity can markedly alter the efficacy of drugs due to altered drug half-life or first-pass metabolism of orally administered drugs (*3*). As such, changes in CYP3A activity are a common cause of detrimental drug−drug interactions.

CYP3A is a relatively unstable protein that has been reported to be stabilized by substrates (*4*), although the precise molecular mechanisms involved in substrate-mediated stabilization have not been elucidated. We recently identified an in vitro incubation system that mimics substrate-mediated stabilization of CYP3A (*5*). We utilized microsomes isolated from the livers of rats that had been treated with nicardipine (Nic), an efficacious inducer of CYP3A protein (*6*). Incubation of these microsomes at 37 °C resulted in a shift of the major ∼55 kDa CYP3A band to HMM bands in a process selective for CYP3A (*5*). The HMM CYP3A was degraded in the presence of cytosol by a mechanism that was not affected by proteasome inhibitors (*5*). Furthermore, although ubiquitin could be identified in immunoprecipitated samples of HMM CYP3A, this ubiquitin apparently resulted from CYP3A aggregating with polyubiquitinated proteins already present in the ER (*5*). That is, formation of these ubiquitin−CYP3A conjugates did not require monomeric ubiquitin, ATP, Mg^{2+}, ubiquitin E1 activating enzyme, or other cytosolic enzymes typically required for a prototypical polyubiquitination reaction (*5*). Furthermore, immunoprecipitated HMM CYP3A appeared to be in molar excess to ubiquitin, a relationship opposite what would be expected of a classical polyubiquitination reaction (*5*). More recently, we found that hemin treatment of primary cultured rat hepatocytes stimulated the formation of HMM CYP3A bands in a process that was independent of proteasome inhibition (*7*). Because hemin treatment did not increase ubiquitin levels in immunoprecipitated CYP3A and because the HMM CYP3A was found predominately in the detergent insoluble fraction of the 10 000 g pellet, the HMM CYP3A likely represented large protein aggregates rather than polyubiquitinated proteins (*7*).

Typically, the P450 catalytic cycle is dependent upon NADPH and NADPH-P450 reductase. Many P450s, however, can undergo a peroxide shunt that eliminates the need for these cofactors (*8*). In this case, the central P450 heme group is directly oxidized by the peroxide. Although many organic hydroperoxides can facilitate this reaction, fatty acid hydroperoxides (FAOOH) have been shown to be able to support microsomal P450 catalysis rates up to ∼6 times those observed in the presence of NADPH (*9*). In addition to providing for an alternative mechanism for substrate metabolism, the peroxide shunt also converts the peroxide moiety of FAOOH to relatively nontoxic alcohols (*10*). In the presence of NADPH and NADPH-P450 reductase, P450 can also catalyze the reductive β-scission of FAOOH (*11*, *12*). As such, P450 can metabolize FAOOH by more than one mechanism, with different metabolites formed by each mechanism.

† Supported by U.S. Public Health Service Grants R01 DK54812 (R.C.Z.) and R01 CA90426 (F.P.G.).

* To whom correspondence should be addressed. Tel: 1-509-376-8596. Fax: 1-509-376-6767. E-mail: richard.zangar@pnl.gov.

‡ Pacific Northwest National Laboratory.

§ Vanderbilt University School of Medicine.

[1] Abbreviations: BSO, buthionine sulfoximine; CuOOH, cumene hydroperoxide; CYP3A, cytochrome P450 3A; EM, erythromycin; ER, endoplasmic reticulum; HMM, high molecular mass; HNE, 4-hydroxynonenal; HpODE, hydroperoxy-10,12-octadecadienoic acid; MDA, malondialdehyde; Nic, nicardipine; NP40, Nonidet P-40; P450, cytochromes P450; SDS−PAGE, sodium dodecyl sulfate polyacrylamide gel electrophoresis.

10.1021/bi0349975 CCC: $25.00
Published on Web 10/09/2003

In the presence of NADPH, O_2, and NADPH-P450 reductase, CYP3A and other P450s can undergo uncoupling that results in the generation of superoxide anion radical or hydrogen peroxide. This activity can result in the development of oxidative stress within hepatocytes under experimental conditions (*13*). In microsomes, the P450 oxidase activity is often inhibited by substrates (*14*−*16*); although in reconstituted systems with purified P450s, substrate addition can increase uncoupling (*17*). It has also been shown that a byproduct of lipid peroxidation, HNE, inactivates P450 in a process that apparently involves HNE reacting directly with the P450 protein without metabolic activation (*18*). Therefore, P450s have a complex relationship with FAOOH in that these enzymes can indirectly stimulate FAOOH formation, can metabolize FAOOH by at least two mechanisms, and are inactivated by FAOOH breakdown products.

In this study, we demonstrate that oxidative stress is a key factor in the formation of HMM CYP3A in incubated microsomes and in a reconstituted system with the purified enzyme. Furthermore, we demonstrate that a FAOOH can support the formation of the HMM CYP3A and that this process is inhibited by CYP3A substrate. We find that HNE adducts are concentrated in the same HMM range as the CYP3A aggregates and that CYP3A substrates blocked the formation of these adducts. Overall, our data suggest that substrate-mediated stabilization is the result of inhibition of CYP3A-dependent activation of lipid hydroperoxides, which in turn prevents covalent modification and aggregation of the CYP3A protein.

MATERIALS AND METHODS

Materials. Powdered rat chow was purchased from Harlan Teklad (Madison, WI). Monoclonal anti-CYP3A1 (mAb p6) was a generous gift from Dr. C. Roland Wolf (Ninewells Hospital and Medical School, Dundee, U.K.). Monoclonal antibodies for ubiquitin and HNE adducts were from Santa Cruz Biotechnology (Santa Cruz, CA) and Oxis International (Portland, OR). Secondary antibodies conjugated to horseradish peroxidase were from Jackson ImmunoResearch (West Grove, PA). SuperSignal West Pico chemiluminescent reagent was from Pierce (Rockford, IL). Purified 9*S* and 13*S* isomers of HpODE and hydroxy-10,12-octadecadienoic acid were obtained from Cayman Chemicals (Ann Arbor, MI). 13*S*-HpODE was also prepared and purified and the concentration was determined (using absorbance at 235 nm) in our laboratory, as described (*19*). The purity and concentration of the 13*S*-HpODE that we synthesized were confirmed by comparison to the commercial 13*S*-HpODE standard by gas chromatography and mass spectrometry (GC-MS) detection (described below). SYPRO ruby was from Bio-Rad (Hercules, CA). Phosphatidylcholine (purified from bovine liver) and phosphatidylserine (purified from porcine brain) were from Avanti Polar Lipids (Alabaster, AL). Purified human cytochrome P450 reductase and HNE were from Calbiochem (San Diego, CA). Human CYP3A4, which was modified on the N terminus to enhance bacterial expression and contained a histidine tag on the C terminus, was expressed in *Escherichia coli* and purified as described previously (*20*, *21*). Other reagents were from Sigma Chemicals (St. Louis, MO).

Measurement of Thiobarbiturate Reactive Lipids. Malondialdehyde (MDA) equivalents were determined as described (*22*, *23*). In brief, samples containing 5 mg protein/mL, 10 mM K_2HPO_4 (pH 7.4), 88 mM KCl, 13 mM thiobarbiturate, 0.0125 N HCl, and 7.5% trichloroacetic acid were incubated for 30 min at 95 °C. After samples had cooled to room temperature, the thiobarbiturate reactive material was extracted with an equal volume of butanol/pyridine (93.7:6.25; v:v) and A_{532} was measured in a Molecular Devices (Sunnyvale, CA) Spectramax 384 microplate reader.

Microsome Incubation Reactions. Hepatic microsomes were prepared from 6 week old male Sprague−Dawley rats that were treated with Nic or vehicle, as described (*6*, *24*). Microsomes were stored as aliquots at −80 °C for over 1 year, unless indicated otherwise. Incubations were undertaken at 37 °C using 75 μg of microsomal protein, 50 mM Tris HCl (pH 7.5), 25 mM sucrose, 150 mM KCl, 2 mM $CaCl_2$, and 3 μM $ZnCl_2$ in a total volume of 50 μL. Reactions were terminated by addition of 50 μL of SDS−PAGE loading buffer (62.5 mM Tris, pH 6.8, 1% SDS, 11% glycerol, 370 μM bromophenol blue, and 0.5% 2-mercaptoethanol) and heated at 65 °C for 5 min. In some cases, a prooxidant mixture of $FeSO_4$ and ascorbic acid (1:4 molar ratio) was added. Lipophilic antioxidants (100 μM) were added to the reaction mixture immediately prior to incubations. These samples and the associated controls contained 1% ethanol. Incubations were also prepared with the hydrophilic antioxidants: 200 μM deferoxamine mesylate (Def), 5 mM dimethylthiourea (DMTU), 5 mM N-acetylcysteine (NAC), 10 mM mannitol, and 1% DMSO. The hydrophilic antioxidants, prooxidants, and associated control incubations lacked additional solvent. Antioxidants and prooxidants were added immediately prior to the start of the 37 °C incubation.

Incubations with Purified Human CYP3A4 and NADPH-P450 Reductase. Purified CYP3A4 (0.5 μM) and NADPH-P450 reductase (0.5 μM) were reconstituted in 40 mM HEPES (pH 7.4, with KOH), 30 mM $MgCl_2$, and a 2:1 mix (m:m) of phosphatidylcholine:phosphatidylserine (10 mg/mL). In some cases, 100 μM clotrimazole (CTZ) or arachidonic acid was added. Incubations were initiated by the addition of the HpODE and placing the samples in a 37 °C heating block. Reactions were then terminated by placing the samples in an ice bath and adding SDS−PAGE loading buffer. Samples were then heated to 65 °C for 5 min, allowed to cool to room temperature, and analyzed for CYP3A4 levels using the immunoblot procedures described below. In the case of cytochrome P450 reductase, levels of this protein were visualized by staining the samples with SYPRO ruby, as described previously (*25*). The bands were imaged and quantified using the fluorescent mode on a Lumi-Imager F1 (Boehringer Mannheim, Indianapolis, IN), with UV activation and a detection cutoff of 600 nm.

Immunoblot Analyses. Immunoblot analyses using reducing SDS−PAGE were performed as described (*5*). To ensure that the 350 mM 2-mercaptoethanol in the final loading buffer was sufficient to disrupt disulfides, tests were undertaken where the loading buffer was prepared with concentrations of dithiothreitol of 100 or 1000 mM, 135 mM iodoacetamide, or 200 mM tributylphosphine. In another test, urea was added to 8 M in the loading buffer to disrupt potential protein aggregates. Eleven μg of microsomal protein was loaded per lane. Immunoblots were blocked in buffered saline (pH 7) containing 0.1% Tween-20 (PBS-T) and 5% milk powder. Antibodies to CYP3A, ubiquitin, and HNE

adducts were diluted 1:10 000 in PBS-T containing 0.1% bovine serum albumin (w:v), and the blots were incubated overnight at room temperature. Blots were then rinsed with PBS-T and incubated with horseradish peroxidase-conjugated secondary antibody diluted 1:5000 in PBS-T containing 5% milk powder. Protein levels were determined using Super-Signal chemiluminescent reagents and were imaged using a Lumi-Imager F1 (Boehringer Mannheim).

Analysis of HpODE Metabolism. Microsomal samples (250 μg protein) were diluted to 250 μL with 0.1 M $NaPO_4$, pH 7.4. HpODE (100 μM) was added (while on ice), followed immediately by the addition of 0.1% acetonitrile (vehicle control) or 10 μM CTZ, 100 μM Nic, or 100 μM erythromycin (EM). Samples were transferred to a 37 °C water bath and incubated for the indicated time periods. The reaction was stopped, and the HpODE was extracted by addition of 4 °C diethyl ether and vortexing of the samples. Following evaporation of the diethyl ether phase under a gentle stream of nitrogen gas, the HpODE was suspended in 100 μL of ethyl acetate and derivatized with 75 μL of *N*-methyl-*N*-trimethylsilyltrifluoroacetamide for 2 h at room temperature. Derivatized samples were separated and detected using an HP6890 gas chromatograph equipped with an HP5973 mass selective detector and a RTX-5MS column from Restek (Bellefonte, PA) that was 30 m × 0.25 mm internal diameter × 0.25df. The oven had an initial temperature of 100 °C for 1 min, ramped at 15 °C/min to 200 °C with a final ramp of 25 °C/min to 300 °C. The injection inlet was in splitless mode at a constant temperature of 210 °C. Head pressure was a constant 25 psi. Volumes of 1.5 μL were injected into a Restek 4 mm internal diameter cyclodouble gooseneck injection liner. Total analysis time was 13.67 min per sample. Standards of the HpODE isomers equivalent to 10, 25, 50, or 100 μM HpODE in the original samples were prepared in duplicate and analyzed by GC-MS at the same time as the microsome samples. Single ion mass analysis was used to quantitate 9*S*- and 13*S*-HpODE, using *m*/*z* of 308 and 167, respectively. Linear standard curves were consistently generated with correlation coefficients (r^2) of 0.96 or higher. In addition, these mass ions were undetectable at the same elution times in microsome samples processed in an identical manner but did not have added HpODE. 9*S*- and 13*S*-hydroxy-10,12-octadecadienoic acid, potential metabolites of corresponding isomers of HpODE, eluted 1−3 min later than the parent compounds and, therefore, did not interfere with analysis of the parent material. As such, this method was suitable for the quantitative analysis of the HpODE isomers.

Statistics. Statistical comparisons were undertaken using SigmaStat 2.0 software (SPSS Science, Chicago, IL). A *t*-test was used to compare levels of a single treatment group with the control group. Other statistical analyses were undertaken using a one way analysis of variance and, when appropriate, followed by a Tukey's analysis. A probability value of <0.05 was used for all analyses.

RESULTS

In Vivo Treatment with Nic Induces Oxidative Stress in Hepatic Microsomes. When freshly isolated microsomes from Nic-treated rats were used, we were unable to reproduce our previous results observed in comparable microsomes that had been stored for more than a year at −80 °C (*5*). That is, freshly isolated microsomes from rats treated with Nic did not form the HMM CYP3A aggregates when incubated at 37 °C. Rather, we determined that storage at −80 °C resulted in a time-dependent increase in this activity (Figure 1). There is some animal to animal variation in the storage time required for the microsomes from the Nic-treated animals to show this response (data not shown). Even so, microsomes stored for a year or more show a relatively stable rate of HMM CYP3A formation that is similar between samples from different animals (*5*). However, microsomes from control animals that have been stored for 3 years or more (data not shown) or subjected to repeated freeze−thaw cycles (*5*) failed to form HMM CYP3A aggregates when incubated under identical conditions as the microsomes from Nic-treated animals. These results indicated that the ability to form HMM CYP3A aggregates is dependent upon extended storage of microsomal samples as well as in vivo treatment with Nic.

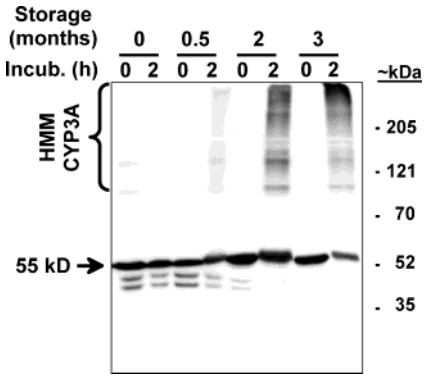

FIGURE 1: Effect of cryostorage on formation of HMM CYP3A aggregates in microsomes from Nic-treated animals. Microsomes prepared from the same Nic-treated animal were stored at −80 °C. The frozen aliquots were subsequently thawed after the indicated storage periods and incubated for 2 h at 37 °C. The sample was then diluted in SDS−PAGE loading buffer and stored at −80 °C until the last sample was collected. After all samples were collected, they were evaluated by immunoblot analysis as described in the Materials and Methods.

P450s are known to catalyze the formation of reactive oxygen species (ROS), and high levels of P450 have been associated with cellular oxidative stress (*13*, *26*). In turn, ROS are known to inactivate proteins, result in protein aggregation, and accelerate protein degradation (*27*). Lipid peroxidation has been reported to increase over time in frozen samples (*28*). Therefore, we suspected that the formation of HMM CYP3A protein activity in frozen microsomes may be the result of lipid peroxidation. To test this hypothesis, thiobarbituric reactive material, a measurement of byproducts formed in the spontaneous degradation of lipid peroxides, was assayed in hepatic microsomes that had been stored for over 1 year at −80 °C without prior thawing and refreezing. These studies indicated that microsomes from Nic-treated rats had a 1.6-fold greater level of lipid peroxidation byproducts as compared to control microsomes (Figure 2). Furthermore, incubation of the microsomes at 37 °C for 30 min increased the amount of reactive lipid products in the microsomes from Nic-treated rats but did not significantly alter levels in control samples. These results indicate that in vivo Nic treatment resulted in a mild oxidative stress in rat

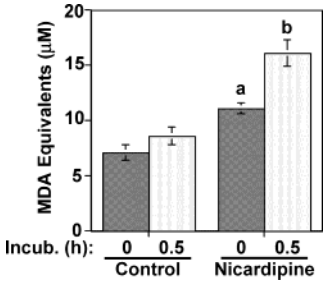

FIGURE 2: Microsomes from Nic-treated rats exhibit elevated levels of lipid hydroperoxide byproducts. Degradative products of lipid hydroperoxides were measured as thiobarbiturate reactive material, as described in the Materials and Methods. The amount of thiobarbiturate reactive material was estimated using MDA as a standard. Each column and crossbar represent the mean and SE, respectively, of the MDA equivalents in the liver microsomes from three animals treated with a control diet or Nic. (a) Value significantly different ($p < 0.05$) from 0 h control values. (b) Value significantly different ($p < 0.05$) from all other samples.

liver and likely depleted antioxidants normally present in the ER membrane.

Oxidative stress can potentially lead to protein aggregation due to disulfide linkages, giving a plausible explanation for the HMM CYP3A bands that we observe. The use of 350 mM 2-mercaptoethanol in the SDS−PAGE loading buffer would normally disrupt these bonds. In addition, we also examined the effects of loading buffer prepared with agents that are more efficacious than 2-mercaptoethanol at breaking disulfide bonds, including 1 M dithiothreitol, 135 mM iodoacetamide, or 200 mM tributylphosphine. These reductants did not have a detectable effect on the amounts of HMM CYP3A present in the incubated microsomes (data not shown). Similarly, 0.5% SDS in the loading and heating is normally sufficient to disrupt protein complexes that are not covalently cross-linked. Still, we used SDS−PAGE loading buffer that also contained 8 M urea to ensure that protein aggregates were dissociated and found that urea addition had no effect on levels of HMM CYP3A detectable in the Western analyses (data not shown). We have also found that 5% SDS is without effect on the level of HMM CYP3A detected in microsomal samples (*7*). It therefore may be that the HMM CYP3A aggregates are the result of protein cross-linking by a mechanism other than disulfide linkages.

Oxidative Stress Leads to Formation of HMM CYP3A Complexes. Oxidative stress was stimulated in hepatic microsomes isolated from three control rats by the addition of iron and ascorbate. Results were compared with those observed with microsomes isolated from three rats treated with 100 mg/kg Nic. Microsomal samples from control animals form HMM CYP3A aggregates only when exposed to the prooxidant mixture, whereas incubation at 37 °C was sufficient to induce aggregation in microsome samples from Nic-treated animals (Figure 3). HNE protein adducts were measured by immunoblot analysis as an indication of lipid peroxidation. Increases in HNE adducts were only detectable in control samples incubated with the prooxidant mixture while microsomes from Nic-treated rats did not require prooxidant treatment for HNE adducts to be detected (Figure 3).

We previously demonstrated that formation of HMM complexes of CYP3A was selective for CYP3A in microsomes from Nic-treated rats (*5*). To see if the same was

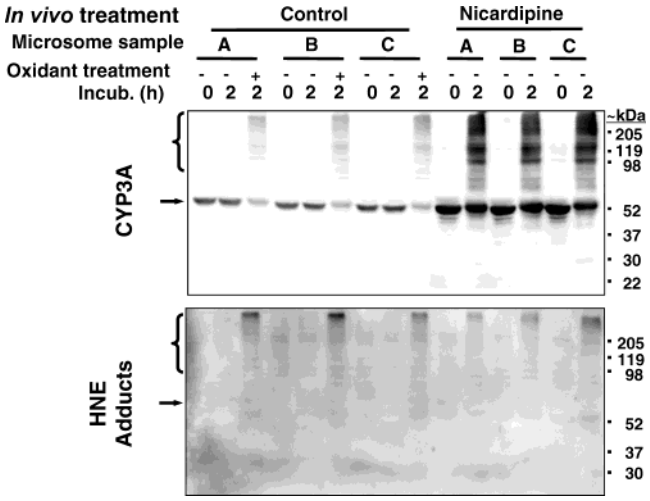

FIGURE 3: Oxidative stress induces the formation of HMM CYP3A and HNE adducts in incubated microsomes from control animals. Hepatic microsomes were isolated from three animals treated with a control diet or three animals treated with 100 mg Nic/day/kg for 7 days. The microsomes were incubated at 37 °C for 0 or 2 h in the presence or absence of an oxidant mixture containing 12.5 μM $FeSO_4$ and 50 μM ascorbic acid. Immunoblots for CYP3A and HNE adducts were then performed as described in the Materials and Methods. The relative positions of monomeric or HMM CYP3A are indicted in both blots by an arrow or bracket, respectively.

true for microsomes from control animals, we compared the effects of varying levels of oxidative stress on CYP3A and the structurally related protein, CYP4A. Increasing oxidative stress progressively increased the conversion of the ~55 kDa CYP3A protein to HMM bands (Figure 4). In contrast, there was no marked effect on CYP4A under any of the test conditions. MDA levels progressively increased with increasing concentrations of the prooxidant mixture, confirming that increased levels of oxidative stress resulted from increasing concentrations of the prooxidant mixture (Figure 4B). Hence, increasing levels of oxidative stress preferentially convert monomeric CYP3A to HMM bands in microsomes from control animals.

Inhibition of CYP3A Aggregation by Antioxidants. If oxidative stress is an important factor in the formation of HMM CYP3A aggregates in microsomes from rats treated with Nic, inhibition by antioxidants would be expected to block this process. The hydrophilic antioxidants Def, DMTU, and NAC partially inhibited the formation of the HMM CYP3A in the incubated microsomes (Figure 5A,B). However, the hydroxy radical scavengers mannitol and DMSO were ineffective, indicating that hydroxy radicals are not required for the formation of the HMM aggregates. Mammalian P450s are membrane proteins with a single N-terminal transmembrane domain and strong contacts between nontransmembrane portions of the protein and the ER surface (*26*). The lipophilic antioxidants were generally more effective than the hydrophilic antioxidants at inhibiting the formation of HMM CYP3A in the incubated microsomes. Lipophilic antioxidants vitamin E (Vit E) and probucol partially inhibited the formation of HMM aggregates while butylated hydroxytoluene (BHT), butylated hydroxyanisole (BHA), and *N*,*N*′-diphenyl-*p*-phenylenediamine (DPPD) completely blocked the formation of HMM aggregates (Figure 5C,D). In all cases, the ability of an antioxidant to inhibit the formation of the HMM CYP3A aggregates was associ-

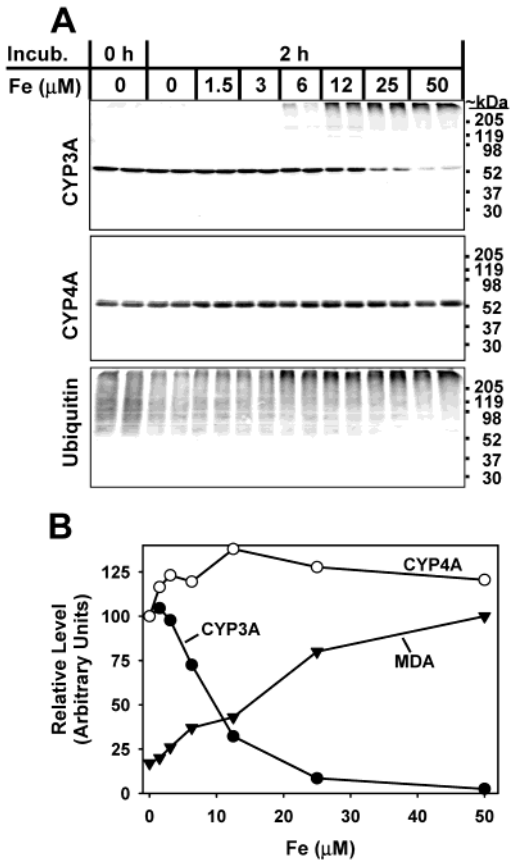

FIGURE 4: Comparison of the effects of oxidative stress on CYP3A, CYP4A, and ubiquitin conjugates in incubated microsomes. Microsomes from vehicle control animals were analyzed by immunoblot prior to incubation (0 h) or after incubation at 37 °C for 2 h in the presence of prooxidant mixture containing 0 to 50 μM iron and ascorbate (at 4× the concentration of the iron), as described in the Materials and Methods. (A) Immunoblot analyses for CYP3A, CYP4A, and ubiquitin. (B) Relative density of the ~55 kDa CYP3A and CYP4A bands shown in panel A (2 h incubations) or the relative amount of thiobarbituric reactive material (MDA equivalents) present after a 30 min incubation.

ated with a comparable decrease in HNE adduct formation (Figure 5).

Because CYP3A substrates inhibit the formation of the HMM CYP3A, we examined some of the antioxidants most effective at preventing HMM CYP3A formation to be sure that they were not CYP3A substrates. These studies indicated that 2 mM BHA and BHT failed to reduce microsomal EM *N*-demethylase while 100 μM CTZ reduced this model CYP3A activity by >99% (data not shown). These results suggest that these compounds alter the formation of HMM CYP3A due to antioxidant effects rather than substrate-mediated stabilization.

HpODE Effects on the Formation of HMM CYP3A in Incubated Microsomes. Lipid hydroperoxides are formed in cells under conditions of oxidative stress and are known to be metabolized by P450s. To determine if lipid hydroperoxides might be a factor in the formation of HMM CYP3A, we incubated microsomes from control rats in the presence or absence of 13*S*-HpODE. HpODE stimulated the formation of HMM CYP3A bands, upward migration of ubiquitin conjugates, and the formation of HNE adducts, similar to that observed in microsomes from Nic-treated rats without

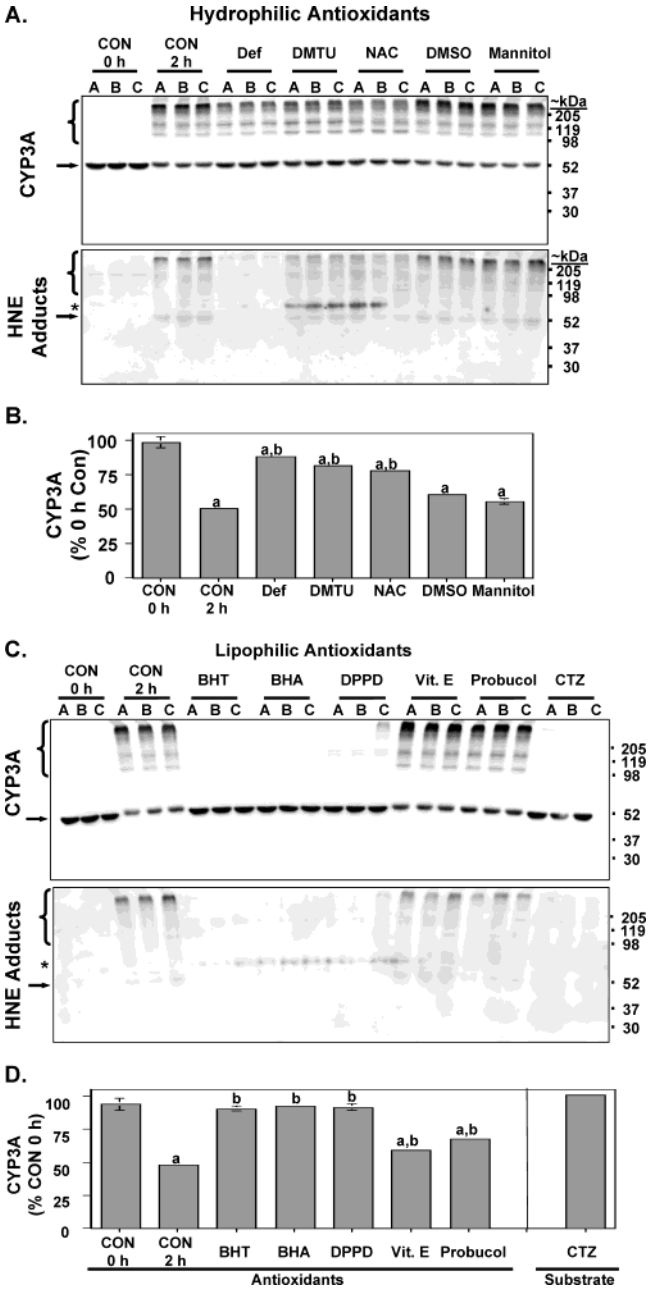

FIGURE 5: Antioxidants inhibit the CYP3A aggregation reaction in microsomes. Microsomes from animals treated with Nic were not incubated (CON 0 h) or incubated at 37 °C for 2 h without added antioxidant (CON 2 h), or in the presence of the indicated antioxidants or the CYP3A substrate, CTZ, as described in the Materials and Methods. The arrow and bracket denote the relative positions of the monomeric ~55 kDa CYP3A and the HMM CYP3A aggregates, respectively. (A) Immunoblots of CYP3A and HNE adducts in the presence or absence of the hydrophilic antioxidants, Def, DMTU, NAC, DMSO, and mannitol. The * indicates the location of an artifact that is occasionally seen with the HNE antibody. (B) Graphical summary of the density of the ~55 kDa CYP3A monomer shown in the immunoblot in panel A. Each column and crossbar represents the mean density and SE, respectively, of three replicate analyses. (C) Immunoblots of CYP3A and HNE adducts in the presence or absence of the lipophilic antioxidants, BHT, BHA, DPPD, Vit E, and probucol, and the CYP3A substrate, CTZ. (D) Graphical summary of the density of the ~55 kDa CYP3A monomer shown in the immunoblot in panel C. Each column and crossbar represent the mean density and SE, respectively, of three replicate analyses. (a) Statistically significant from the 0 h control values. (b) Statistically significant from the 2 h control values.

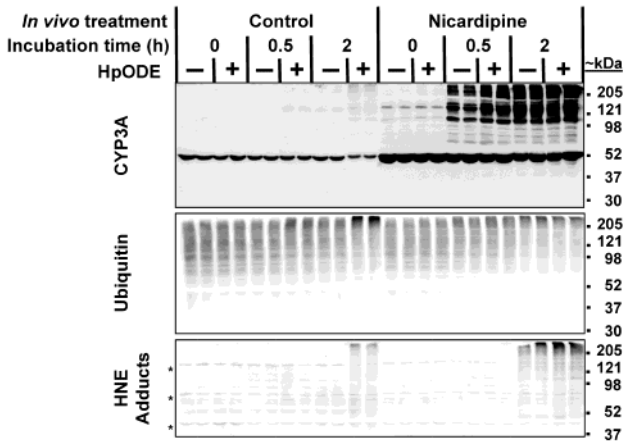

FIGURE 6: HpODE stimulates the formation of HMM CYP3A aggregates in incubated microsomes. Microsomes from dietary control or Nic-treated rats were incubated for 0, 0.5, or 2 h in the presence or absence of 100 μM 13*S*-HpODE. Immunoblot analyses for CYP3A, ubiquitin, and HNE adducts were undertaken as described in the Materials and Methods. The * indicates nonspecific bands seen with the HNE antibody.

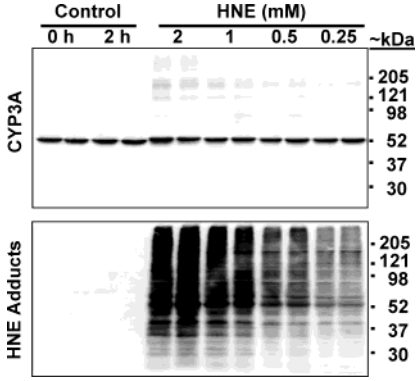

FIGURE 7: Effects of HNE on CYP3A aggregation in incubated microsomes. Microsomes from control rats were not incubated (0 h control) or were incubated for 2 h in the absence of HNE (2 h control) or in the presence of the indicated concentrations of HNE. Immunoblot analyses for CYP3A protein and HNE protein adducts were undertaken as described in the Materials and Methods.

HpODE treatment (Figure 6). In microsomes from Nic-treated rats, addition of HpODE slightly accelerated the formation of the HMM CYP3A, as seen at the 30 min time point (Figure 6). However, at 2 h, HpODE had no discernible effect in the microsomes from Nic-treated rats.

HNE Effects on the Formation of HMM CYP3A in Incubated Microsomes. HNE has been reported to cross-link proteins (*29*), and increases in HNE adducts were consistently observed in experiments described in this paper under conditions that resulted in the formation of HMM CYP3A. Therefore, we added varying concentrations of HNE directly to microsomes from control rats and determined effects on levels of HMM CYP3A complexes. These concentrations of HNE were higher than would be expected to occur in the incubated microsomes (*30*). Therefore, if HNE was a key factor in the formation of HMM CYP3A, these concentrations should be sufficient to stimulate this process. A concentration-dependent increase in HMM CYP3A adducts was observed with the addition of HNE (Figure 7), but levels of HMM CYP3A were much lower than previously observed in microsomes from Nic-treated animals or control microsomes treated with various prooxidants. Although there

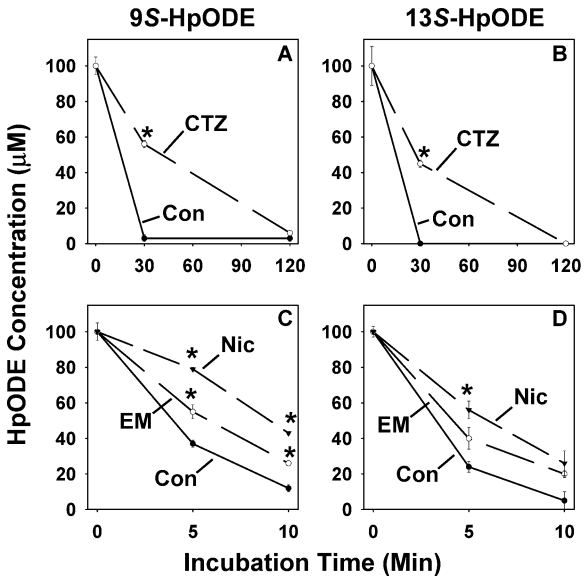

FIGURE 8: Effects of CYP3A substrates on the loss of HpODE in incubated microsomes. Microsomes were incubated in the presence of the 9*S* or 13*S* isomer of HpODE for the times indicated. CYP3A substrates, 10 μM CTZ, 100 μM EM, or 100 μM Nic were added as indicated. Levels of HpODE were determined after the indicated incubation time by GC-MS, as described in the Materials and Methods. Each data point and crossbar represent the mean and SE of three individual samples. *Statistically significant from control samples at the same time point.

were exceptionally high levels of HNE adducts detected, the pattern of HNE adduction was much different than observed in the previous experiments. That is, direct addition of HNE appeared to generally label proteins while addition of prooxidants resulted in HNE adducts concentrated in the same HMM region that CYP3A aggregates are observed. These data suggest that HNE resulting from oxidative stress preferentially binds to the proteins that form the HMM complexes but that direct addition of HNE itself is ineffective at stimulating formation of HMM CYP3A.

CYP3A Substrate Effects on the Loss of HpODE in Incubated Microsomes. CTZ, a CYP3A substrate, was found to effectively inhibit the formation of the HMM CYP3A in incubated microsomes (Figure 5C), consistent with our previous studies (*5*). Interestingly, CTZ also blocked HNE adduct formation (Figure 5C). These data suggest that CYP3A catalytic activity may contribute to oxidative stress and the formation of the HNE adducts, possible through the catalytic activation of lipid hydroperoxides. Therefore, we determined the loss of HpODE isomers in microsomes from rats treated with Nic. These microsomes had been isolated within 2 months of use.

In an initial study, microsomes were incubated for 0.5 or 2 h in the presence of 9*S*- or 13*S*-HpODE with or without the addition of CYP3A substrate. In the absence of substrate, both isomers of HpODE were rapidly degraded and were essentially undetectable after a 30 min incubation (Figure 8A,B). When CTZ was added to these samples, this loss of HpODE was markedly reduced, such that ~50% of both HpODE isomers remained after a 30 min incubation (Figure 8A,B). However, when EM or Nic was added, essentially no HpODE remained after 30 min (data not shown). To determine if, like CTZ, these two CYP3A substrates inhibited the loss of HpODE in the incubated microsomes, effects were

examined at earlier time points (i.e., 5 and 10 min) when HpODE metabolism was incomplete. These studies confirmed the rapid loss of HpODE, such that by 5 min, less than 40% of either isomer remained (Figure 8C,D). The addition of Nic or EM decreased the rate of loss of HpODE, confirming that CYP3A substrates generally inhibit the metabolism of HpODE.

Studies with Purified CYP3A4. Studies were undertaken using purified human CYP3A4 that was reconstituted with phospholipid but without other proteins or cofactors. This mixture was incubated in the presence or absence of 50 mM HpODE for 0.5 or 2 h. In the absence of HpODE, the enzyme did not form HMM complexes, as demonstrated in the silver-stained, SDS−PAGE gel (Figure 9A). The addition of 50 mM HpODE resulted in the formation of HMM CYP3A4 within 30 min (Figure 9A). Subsequent studies indicated that HpODE stimulation of HMM CYP3A4 was essentially complete within 10 min of incubation time (data not shown). Therefore, the reconstituted CYP3A4 was much more stable in the absence of HpODE.

A second study was undertaken in which the samples were analyzed for the presence of HNE adducts after 10 or 30 min incubations. In the regular reconstitution system, which lacked free fatty acids, levels of HNE adducts were near the limit of detection regardless of whether HpODE was added, although slight increases in HNE adducts were observed in the presence of HpODE (Figure 9B). The addition of arachidonic acid to the incubation mixture markedly increased the levels of HNE adducts. We also found that addition of a CYP3A4 substrate, CTZ, partially blocked the formation of the HMM CYP3A4 bands and the associated loss of the ~55 kDa band (Figure 9C). When cytochrome P450 reductase was also added to the mixture, HpODE resulted in a concentration-dependent reduction of the 55 kDa CYP3A4 band but had little effect on the NADPH-P450 reductase, suggesting that the HpODE preferentially induced the formation of HMM CYP3A4 bands (Figure 9D).

DISCUSSION

We have previously demonstrated that HMM CYP3A−ubiquitin conjugates are formed in incubated microsomes in a process that appears to be independent of a classical polyubiquitination reaction (*5*). In this study, we examined the role of oxidative stress in stimulating the formation of the HMM CYP3A in incubated microsomes and primary cultured rat hepatocytes. We found increased levels of byproducts of lipid hydroperoxides in microsomes from Nic-treated rats, suggesting a link between oxidative stress and the generation of HMM CYP3A. This hypothesis was further supported by studies that showed that prooxidants stimulated the formation of the HMM CYP3A in microsomes from control animals and that antioxidants blocked this process in microsomes from animals treated with Nic. Given that the P450 can metabolize FAOOH by multiple mechanisms, we speculated that effects of oxidative stress on CYP3A protein stability may be mediated by direct interaction with FAOOH. Indeed, addition of HpODE was sufficient to stimulate the formation of the HMM CYP3A aggregates in microsomes from control animals that otherwise lacked this activity and in a reconstituted system containing CYP3A4.

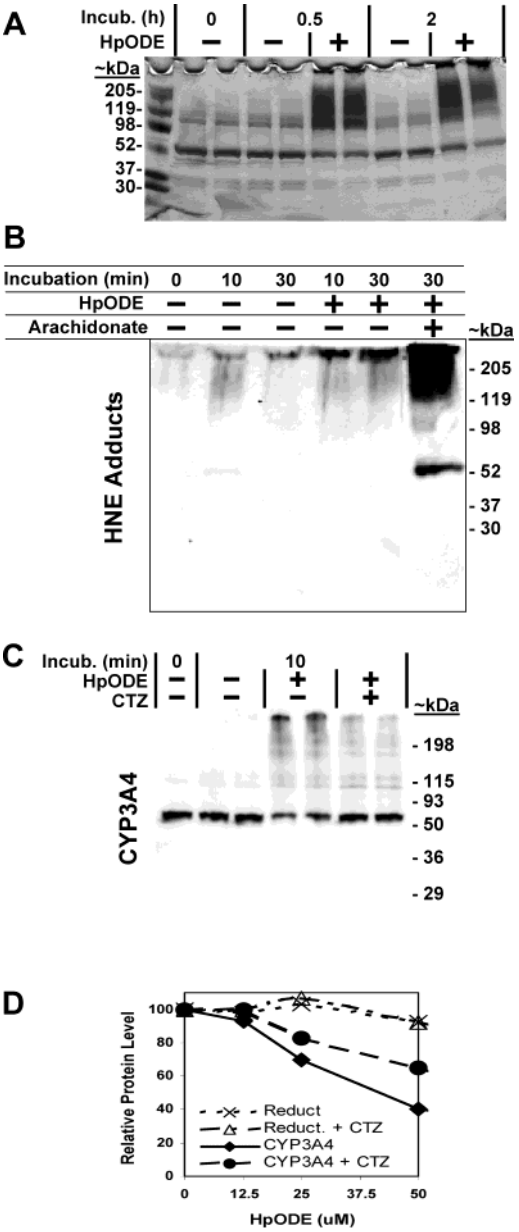

FIGURE 9: HpODE effects on reconstituted human CYP3A4. Purified CYP3A4 was reconstituted with phospholipids as described in the Materials and Methods. (A) Silver-stained SDS−PAGE gels of samples that contained purified CYP3A4 that had been incubated for 0.5 or 2 h with or without the addition of 50 μM 13*S*-HpODE. (B) Immunoblot analysis of HNE adducts present in samples of purified CYP3A4 that had been incubated for 10 or 30 min in the presence or absence of 50 mM 13*S*-HpODE. Arachidonic acid (100 μM) was also added to one sample incubated for 30 min. (C) Immunoblot analysis in samples that contained purified CYP3A4. Samples had been incubated for 0 or 10 min with or without the addition of 50 μM 13*S*-HpODE and 100 μM CTZ. (D) Concentration-dependent effects of HpODE on the monomeric bands of CYP3A4 and cytochrome P450 reductase. CYP3A4 levels were determined by immunoblot analysis, while cytochrome P450 reductase levels were determined by the fluorescence intensity of bands stained with SYPRO ruby, as described in the Materials and Methods. Samples were incubated for 10 min in the presence of 0, 12.5, 25, or 50 μM HpODE and the presence or absence of 100 μM CTZ.

Studies with inhibitors confirmed that CYP3A does rapidly metabolize HpODE and that this activity is inhibited by CYP3A substrates. Overall, these results suggest that the affinity of CYP3A for FAOOH increases the susceptibility

of this enzyme to protein aggregation in response to oxidative stress.

P450s catalyze a reductive β-scission of FAOOH that is NADPH dependent (*11*, *12*). For some P450s (e.g., CYP2E1[2]), the molar production of two metabolites (pentane and either an aldehyde or a hydroxy acid) was nearly equal to the amount of the FAOOH metabolized or NADPH consumed. However, for CYP3A6[1], no more than 40% of the parent compound could be accounted for by these products. Our study differs substantially from these previous studies (*11*, *12*) in that we did not add NADPH to our reaction mixture. In the absence of NADPH, arachidonic acid hydroperoxide can be metabolized by P450 to a variety of epoxyalcohols (*32*), although the proportion of these products relative to total metabolism is unclear. Therefore, we cannot currently conclude what the major metabolites produced by CYP3A metabolism of FAOOH are. Although it is clear that some HNE is formed in our incubation system, this compound may be a nonenzymatic byproduct of other metabolites. Because HNE is known to react with and inactivate P450s without metabolic activation by the P450s (*18*), the formation of this compound in our system can be expected to inactivate the protein.

A series of tests with antioxidants suggested a correlation between the level of HNE adducts and the formation of HMM CYP3A (Figure 5). It is particularly relevant that the HNE adducts formed tended to be in the very HMM range. We have previously analyzed this section of the gel using in-gel trypsin digestion and mass spectrometry (*5*). This analysis indicated that prior to incubation at 37 °C, the microsomes had exceptionally low levels of protein in this HMM region of the gel. After incubation, CYP3A was found at easily detectable levels in the HMM region and likely was the most abundant protein present. Therefore, the presence of HNE adducts in the HMM range suggests that HNE is preferentially binding to the protein aggregates, possible prior to aggregation, and may be binding to CYP3A itself.

In studies where HNE was added directly to the microsomes, HNE adducts were detected in a diverse, nonspecific pool of proteins and did little to stimulate the formation of HMM CYP3A. Therefore, HNE may not exhibit an inherent preference for binding to CYP3A or HMM proteins as compared to other microsomal proteins. For this reason, we speculated that HNE preferentially binds to CYP3A in the incubated microsomes because this compound is formed in close proximity to this protein as a result of CYP3A metabolism of HpODE. Studies with purified enzymes, however, demonstrated that HMM CYP3A4 bands were formed even when only trace amounts of HNE adducts were detectable. The addition of arachidonic acid to the reconstituted CYP3A4 increased levels of HNE adduct formation. This result suggests that there is a propagation of the lipid peroxidation in the presence of arachidonic acid and that the formation of HNE adducts is primarily dependent upon the oxidation of arachidonic acid and subsequent degradation to HNE. According to the manufacturer, the HNE antibody that we used will only recognize 1:1 HNE:amino acid (Michael) adducts and does not recognize amino acids cross-linked by HNE or single adducts of other HpODE breakdown products such as *trans*-2-nonenal, *trans*-2-pentenal, MDA, or acrolein. Therefore, although our data strongly suggest that metabolism of FAOOH is a key factor in the formation of the HMM CYP3A bands, the studies presented here are insufficient to determine whether protein adduction or cross-linking by HpODE breakdown products are important in this process. It may also be that the reason that we do not detect HNE adducts in the presence of C_{18} HpODE is that HpODE metabolism leads to reactive byproducts that are shorter than C_9 HNE formed in the presence of C_{24} arachidonic acid hydroperoxide. If so, it may be that these shorter degradative products of HpODE are equally capable as HNE of stimulating the formation of the HMM CYP3A4.

We have previously observed in microsomes from Nic-treated animals that the formation of HMM CYP3A is a selective process, such that the most abundant protein in the HMM range appears to be CYP3A (*5*). In the current study, we find that oxidative stress also preferentially stimulates the formation of HMM CYP3A as compared to a related protein, CYP4A (Figure 4). Using a reconstituted system containing CYP3A4 and NADPH-P450 reductase, we found that CYP3A4 more readily forms HMM aggregates than the reductase (Figure 9D). Therefore, we conclude that although oxidative stress is likely to affect many proteins, CYP3A is particularly susceptible to protein aggregation in response to lipid hydroperoxides.

We have previously noted that in the incubated microsomes, CYP3A appears to form dimers or trimers with itself prior to forming the larger complexes that are observed in immunoblots as a general smear above 200 kDa (*5*). Notably, we immunoprecipitated the potential CYP3A trimer and analyzed it by in-gel tryptic digestion and tandem mass spectrometry (*5*). We were only able to identify peptides from CYP3A proteins in this analysis, consistent with the concept that this band was a homotrimer (*5*). In this study, we found that HpODE stimulates purified CYP3A4 to form aggregates with itself, clearly demonstrating that other proteins are not necessary for the formation of the HMM CYP3A (Figure 9). In reconstituted proteoliposomes, P450s proteins have been observed to form oligomers (*33*) and immunoelectron microscopy has suggested that P450s are not randomly distributed but are clustered in close proximity (*34*, *35*). Adjacent P450s may preferentially aggregate even if this process was otherwise not highly specific. Therefore, we speculate that the initial step in the formation of the HMM CYP3A complexes is aggregation of CYP3A protein to itself.

Overall, the results of this and other studies suggest a mechanism regulating CYP3A protein stability, which is diagrammed in Figure 10, that has not previously been reported for the P450 superfamily. Nic treatment of rats induces high levels of CYP3A expression (step 1). CYP3A oxidase activity generates ROS (step 2) that nonenzymatically stimulate lipid peroxidation (step 3). Our data suggest that this oxidase activity occurs in vivo and thereby predisposes an increase in oxidative lipid damage in the microsomes from the Nic-treated animals. There should not be oxidase activity in the incubated microsomes, since these incubates lack NADPH. The lipid hydroperoxides are themselves metabolized by CYP3A, thereby producing reactive lipid products (step 4). These reactive products rapidly adduct to CYP3A (step 5) and then either directly

[2] In the manuscript by Vaz et al. (*11*), CYP3A6 is referred to as the "3c" form, while CYP2E1 is referred to as the "3a" form, based on a list of early P450 nomenclature (*31*).

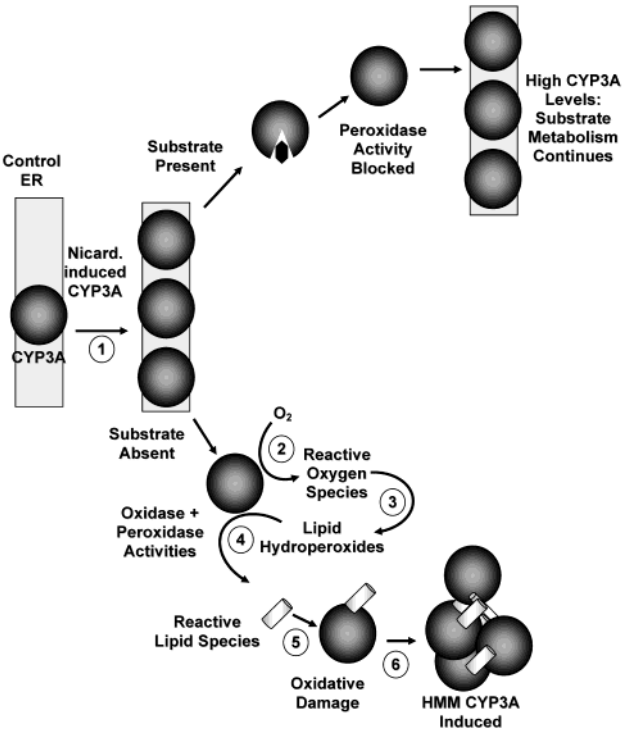

FIGURE 10: Schematic diagram of proposed mechanism by which substrates stabilize CYP3A protein. Numbers indicate various steps referred to in the Discussion.

cross-link CYP3A proteins or stimulate protein unfolding that leads to β-aggregation (step 6). This process primarily generates oligomers of CYP3A, but complexes with other microsomal proteins are also formed. The end result of this process is a reduction of the CYP3A activity and the associated oxidative stress. In the presence of substrate, the P450's ability to metabolize lipid hydroperoxides is inhibited (upper pathway). As such, it is possible that this mechanism may selectively reduce P450 species that lack substrate while preserving levels of P450s that are catalytically important.

REFERENCES

1. Nelson, D. R., Koymans, L., Kamataki, T., Stegeman, J. J., Feyereisen, R., Waxman, D. J., Waterman, M. R., Gotoh, O., Coon, M. J., Estabrook, R. W., Gunsalus, I. C., and Nebert, D. W. (1996) *Pharmacogenetics 6*, 1−42.
2. Bertz, R. J., and Granneman, G. R. (1997) *Clin. Pharmacokinet. 32*, 210−258.
3. Thummel, K. E., and Wilkinson, G. R. (1998) *Annu. Rev. Pharmacol. Toxicol. 38*, 389−430.
4. Watkins, P. B., Bond, J. S., and Guzelian, P. S. (1987) Degradation of the hepatic cytochromes P-450. in *Mammalian Cytochromes P-450* (Guengerich, F. P., Ed.) Vol. II, pp 173−192, CRC Press, Boca Raton, Florida.
5. Zangar, R. C., Kimzey, A. L., Okita, J. R., Wunschel, D. S., Edwards, R. J., Kim, H., and Okita, R. T. (2002) *Mol. Pharmacol. 61*, 892−904.
6. Zangar, R. C., Okita, J. R., Kim, H., Thomas, P. E., Anderson, A., Edwards, R. J., Springer, D. L., and Okita, R. T. (1999) *J. Pharmacol. Exp. Ther. 290*, 1436−1441.
7. Zangar, R. C., Kocarek, T. A., Shen, S., Bollinger, N., Dahn, M., and Lee, D. W. (2003) *J. Pharmacol. Exp. Ther. 290*, 1436−1441.
8. Hollenberg, P. F. (1992) *FASEB J. 6*, 686−694.
9. Anari, M. R., Khan, S., Jatoe, S. D., and O'Brien, P. J. (1997) *Eur. J. Drug Metab. Pharmacokinet. 22*, 305−310.
10. Kupfer, R., Liu, S. Y., Allentoff, A. J., and Thompson, J. A. (2001) *Biochemistry 40*, 11490−11501.
11. Vaz, A. D., Roberts, E. S., and Coon, M. J. (1990) *Proc. Natl. Acad. Sci. U.S.A. 87*, 5499−5503.
12. Coon, M. J., Vaz, A. D., and Bestervelt, L. L. (1996) *FASEB J. 10*, 428−434.
13. Puntarulo, S., and Cederbaum, A. I. (1998) *Free Radical Biol. Med. 24*, 1324−1330.
14. Leclercq, I. A., Farrell, G. C., Field, J., Bell, D. R., Gonzalez, F. J., and Robertson, G. R. (2000) *J. Clin. Invest. 105*, 1067−1075.
15. Ekstrom, G., and Ingelman-Sundberg, M. (1989) *Biochem. Pharmacol. 38*, 1313−1319.
16. Persson, J. O., Terelius, Y., and Ingelman-Sundberg, M. (1990) *Xenobiotica 20*, 887−900.
17. Davydov, D. R. (2001) *Trends Biochem. Sci. 26*, 155−160.
18. Bestervelt, L. L., Vaz, A. D., and Coon, M. J. (1995) *Proc. Natl. Acad. Sci. U.S.A. 92*, 3764−3768.
19. Gibian, M. J., and Vandenberg, P. (1987) *Anal. Biochem. 163*, 343−349.
20. Gillam, E. M., Baba, T., Kim, B. R., Ohmori, S., and Guengerich, F. P. (1993) *Arch. Biochem. Biophys. 305*, 123−131.
21. Hosea, N. A., Miller, G. P., and Guengerich, F. P. (2000) *Biochemistry 39*, 5929−5939.
22. Debri, K., Boobis, A. R., Davies, D. S., and Edwards, R. J. (1995) *Biochem. Pharmacol. 50*, 2047−2056.
23. Ohkawa, H., Ohishi, N., and Yagi, K. (1979) *Anal. Biochem. 95*, 351−358.
24. Okita, J. R., Castle, P. J., and Okita, R. T. (1993) *J. Biochem. Toxicol. 8*, 135−144.
25. Berggren, K., Chernokalskaya, E., Steinberg, T. H., Kemper, C., Lopez, M. F., Diwu, Z., Haugland, R. P., and Patton, W. F. (2000) *Electrophoresis 21*, 2509−2521.
26. Goeptar, A. R., Scheerens, H., and Vermeulen, N. P. (1995) *Crit. Rev. Toxicol. 25*, 25−65.
27. Squier, T. C. (2001) *Exp. Gerontol. 36*, 1539−1550.
28. Yan, P. S. (1999) *Adv. Exp. Med. Biol. 459*, 79−98.
29. Requena, J. R., Fu, M. X., Ahmed, M. U., Jenkins, A. J., Lyons, T. J., Baynes, J. W., and Thorpe, S. R. (1997) *Biochem. J. 322* (Pt. 1), 317−325.
30. Esterbauer, H., Schaur, R. J., and Zollner, H. (1991) *Free Radical Biol. Med. 11*, 81−128.
31. Nelson, D. R., Kamataki, T., Waxman, D. J., Guengerich, F. P., Estabrook, R. W., Feyereisen, R., Gonzalez, F. J., Coon, M. J., Gunsalus, I. C., and Gotoh, O. (1993) *DNA Cell Biol. 12*, 1−51.
32. Chang, M. S., Boeglin, W. E., Guengerich, F. P., and Brash, A. R. (1996) *Biochemistry 35*, 464−471.
33. Myasoedova, K. N., and Magretova, N. N. (2001) *Biosci. Rep. 21*, 63−72.
34. Matsuura, S., Fujii-Kuriyama, Y., and Tashiro, Y. (1978) *J. Cell Biol. 78*, 503−519.
35. Schwarz, D., Kruger, V., Chernogolov, A. A., Usanov, S. A., and Stier, A. (1993) *Biochem. Biophys. Res. Commun. 195*, 889−896.

BI0349975